arXiv:1301.5920v1 [cond-mat.mes-hall] 24 Jan 2013

Tunable adsorbate-adsorbate interactions on graphene

Dmitry Solenov,[1,*] Chad Junkermeier,[1] T. L. Reinecke,[1] and Kirill A. Velizhanin[2,†]
[1] *Naval Research Laboratory, Washington, District of Columbia 20375, USA*
[2] *Theoretical Division, Los Alamos National Laboratory, Los Alamos, NM 87545, USA*

We propose mechanisms to control the interaction between adsorbates on the surface of graphene. We show that the interaction between a pair of adsorbates—the change in adsorption energy of one adsorbate in the presence of another—is dominated by a non-linear exchange interaction mediated by graphene's π-electrons. *Ab initio* density functional, numerical tight-binding, and analytical calculations are used to develop the theory. We demonstrate that the interaction can be tuned in a wide range (up to complete reversal) of values as a function of distance by adjusting the adsorbate-graphene bonding or the chemical potential.

Graphene is a one-atom-thick sheet of carbon. It is of interest for a variety of applications ranging from transport to photovoltaics and DNA manipulations [1–3], and has potential to become a successor to silicon in micro- and nanoelectronic applications. The unique electronic transport properties of graphene are rooted in its two-dimensional honeycomb carbon network structure. However, wider applications are limited by difficulties in opening a bandgap and its lack of processability. Both of these limitations can be addressed through chemical modifications [4]. Recently, the range of potential applications has been enlarged by recognizing that chemical functionalization [5–7] of graphene can change its electronic, chemical, and mechanical properties, tailoring them to meet specific needs. As a result, design and control of functionalization has become an important challenge.

Atoms or molecules near the surface of graphene can adsorb via Van-der-Waals interaction (physisorption) or by forming chemical bonds with one or several carbon atoms on the surface (chemisorption). Chemical functionalization of graphene is typically based on chemisorbed atoms or molecules that remain chemically active or provide other functions, e.g., influence conductance when adsorbed in large numbers. Adsorbate-graphene interaction for various types of adsorbates have been discussed in literature [8–16]. Recently, it has been recognized that adsorption energy of an adsorbed atom or molecule can depend strongly on the presence of other adsorbates in its vicinity. The adsorbate-adsorbate (A-A) interaction becomes especially important at large concentrations of adsorbates, affecting both stability and aggregation when forming functionalized surfaces [17–21]. Therefore, understanding the nature of the A-A interaction is a key to design and control of functionalization of graphene.

In this Letter we investigate the microscopic mechanisms underlying the interaction between two atoms or molecules adsorbed on graphene at a distance from each other. We demonstrate that A-A interaction is dominated by an exchange interaction mediated by graphene's π-electrons. We show that A-A interactions can be modified up to complete reversal of sign by changing the chemical potential or the adsorbate-graphene bonding. We use a combination of first-principles density functional theory (DFT) calculations [22], numerical tight-binding (TB), and analytical functional integral approach to identify the role of different microscopic mechanisms responsible for the interaction. We illustrate the approach using fluorine adsorbates as an example relevant to a variety of applications, and demonstrate how our analysis applies to more complex systems.

Chemisorbed atoms or molecules can form one (monovalent) or several (multivalent) bonds with the carbon (C) atoms of the graphene lattice. Monovalent adsorbates, e.g., fluorine (F), adsorb on top of one of the C atoms forming (typically) a mixed covalent-ionic bond. In the case of F the covalent component of the bond is formed by the overlap of F *pz*-orbital (z-axis perpendicular to the grahene's plane) and *s*-*pz* hybridized orbital of C atom. The C atom participating in the bond changes its hybridization from sp^2 to sp^3 taking one *pz* electron out of the π-system. This does not completely remove the amplitude for the electron to hop to the fluorine-carbon complex, but instead it leads to creation of a more complex state near each adsobate site as well as a local deformation of graphene. These modifications can lead to four possible A-A interaction mechanisms: (i) direct overlap of adsorbate's electron orbitals if two adsorbed atoms are in direct contact with each other; (ii) gain or loss of energy due to change of elastic deformation energy of the graphene sheet when two adsorbates are nearby; (iii) Coulomb interaction between excess charges drawn to each adsorbate; (iv) interaction induced by multiple scattering of graphene's π-electrons off the adsorption sites. The first contribution is effective only for atoms adsorbed in direct proximity from each other [23]. Lattice deformations can be demonstrated to produces $1/r^3$ contribution (see also [24, 25]) that is weak $\sim 1-10$ meV, except at the shortest distances. In what follows we demonstrate that the primary contribution to A-A interaction at larger distances comes from the interplay between Coulomb and scattering-induced, or electron exchange, interactions.

The Coulomb and electron exchange interactions in the system of two adsorbates on graphene can be described by a TB Hamiltonian [28] of the form

$$H=-\sum_{\langle ij\rangle'} t c_i^\dagger c_j+\sum_{n=1,2;s} u_{n,s} a^\dagger_{n,s} a_{n,s}-\sum_{\langle in\rangle,s} t'_{n,s}(c_i^\dagger a_{n,s}+a^\dagger_{n,s} c_i)$$
$$+\sum_{i\neq j}\frac{U_{i,j}}{2}\hat{n}_i\hat{n}_j+\sum_{i,n=1,2;s} U^{(s)}_{i,n}\hat{n}_i\hat{\mathfrak{n}}_{n,s}+\sum_{s,s'}\frac{\bar{U}^{(s,s')}_{1,2}}{2}\hat{\mathfrak{n}}_{1,s}\hat{\mathfrak{n}}_{2,s'}. \quad (1)$$

Here the first term describes graphene's π-electrons [26, 27], the $c_i^\dagger$ (c_j) are creation (annihilation) operators of pz states on C atoms [29], and t is the hopping integral between the nearest pz states. The adsorbates (numbered by $n = 1, 2$) can form chemical bonds with several nearby carbon atoms removing their pz states from the graphene's π-system, as indicated by the prime in $\langle ij\rangle'$. Each bonded adsorbate-carbon complex (ACC) can have several states, as indicated by s in the second term of (1). The hopping integrals between ACC states and pz states on other C atoms is denoted by $t'_{n,s}$ in the third term of (1). The creation (annihilation) operators for s-th ACC state are $a^\dagger_{n,s}$ ($a_{n,s}$). The fourth term of (1) is the Coulomb interaction between the π-electrons ($\hat{n} = c^\dagger c$). The fifth term represents the Coulomb interaction between the π-electrons and electrons that occupy ACC states ($\hat{\mathfrak{n}} = a^\dagger a$). Finally, the sixth term is the Coulomb interaction energy between electrons on the two ACCs.

The parameters u and t' of the Hamiltonian (1) are not known. They can be obtained from experiment or from DFT calculations [22, 30–33] by analyzing the density of states (DOS) of graphene with a *single* adsorbate. We will consider F as the adsorbate to illustrate this parametrization. Fluorine bonds to one carbon atom. The two states that are closest in energy to graphene's Dirac point and are sufficiently connected by tunneling to π-electrons are the bonding (symmetric) and the antibonding (antisymmetric) overlap of pz orbitals of C and F. These states can be identified in the projected DOS (PDOS), as shown in Fig. 1(a). In the case of F, it is suffisient to consider only the anti-bonding state in the TB description. In this case s in Eq. (1) takes a single value an will be omitted.

To extract the values of u and t' we compute the TB DOS [34] for one adsorbate based on the first three terms of (1). The resulting DOS [see Fig. 1(b)] has two peaks associated with the adsorbate: one near the Dirac point and one at higher energies $\sim u$. The former is due to the "missing" (sp^3-hybridized) carbon atom which is now a part of ACC. The non-zero tunneling between this state and the state of the C-F complex at $\sim u$ shifts their energies away from one another. This shift can be obtained analytically in the limit of linear dispersion relation as $\varepsilon(\varepsilon - u) = \pi\sqrt{3}t'^2/2 \log|3^{1/4}\sqrt{\pi}t/\varepsilon|$. For small t', the two energy branches can be approximated as $\varepsilon \approx u \pm \sqrt{u^2 + (3t'/2)^2}/2$ which can be understood on the basis of a simple model of two states connected via tunneling amplitude t'. In order to track the shift due to t' we compute DFT DOS [30] for graphene sheet with one missing carbon atom, which corresponds to $u \to \infty$ and $t' = 0$. Comparing DFT and TB results we obtain $t' \approx 0.27t$ and $u \approx 0.75t$. The parametrization for other types of adsorbates can be done similarly.

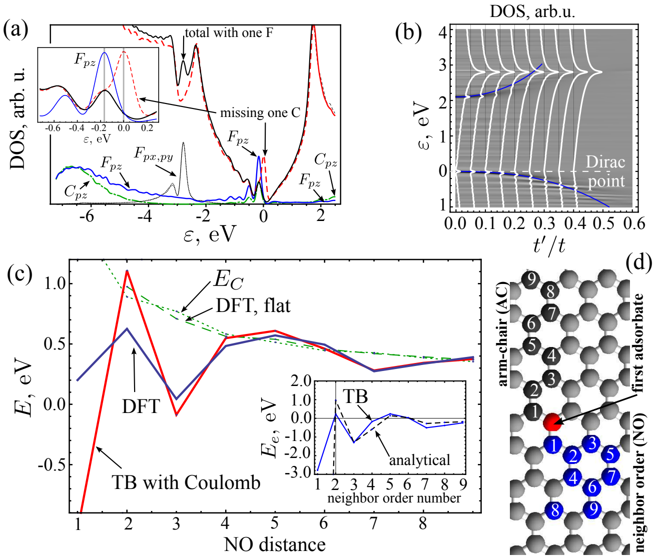

Figure 1: The results of DFT, TB, and analytical calculations. (a) DFT DOS and projected DOS (PDOS) for the system of graphene with a *single* adsorbed F and clean graphene with one missing C atom. The bonding and anti-bonding states of the F-C complex can be identified as buildup of PDOS (projected on pz states of F and C) above and below the Dirac point. The inset magnifies the Dirac point region and shows the shift of the DOS peak due to non-zero t'. (b) TB DOS as a function of t'. The two solid (blue) curves are the analytical solution to the energies of the adsorbate states as discussed in the text. The white curves are total DOS (the reference point for each curve is shown by a vertical line). The background density plot represents the difference between TB DOS with and without F atom: the two main peaks (darker shade) follow the analytical solution for small-to-intermediate values of t'/t. (c) Interaction energy between two F's as a function of neighbor order distance as shown in panel (d), see the text for discussion. (d) Numbering convention for the distance (positions) between the two adsorbates: one adsorbate is at position "0" (red) and the other is at any of the other marked sites.

The energy of the system of *two* adsorbates on graphene, $\mathcal{E}(\mathbf{R})$, described by (1) as a function of the distance $\mathbf{R} = \mathbf{R}_2 - \mathbf{R}_1$ between the two adsorbates can be separated into three components: the energy of graphene with two adsorbates at $R = \infty$, $\mathcal{E}(\infty)$, the energy of Coulomb interaction between adsorbates, $E_C(\mathbf{R})$, and the electron scattering-induced interaction energy $E_e(\mathbf{R})$, i.e. $\mathcal{E}(\mathbf{R}) = \mathcal{E}(\infty) + E(\mathbf{R})$, where the A-A interaction energy is $E(\mathbf{R}) = E_C(\mathbf{R}) + E_e(\mathbf{R})$. In the case of a simple adsorbate, such as F, the energy of

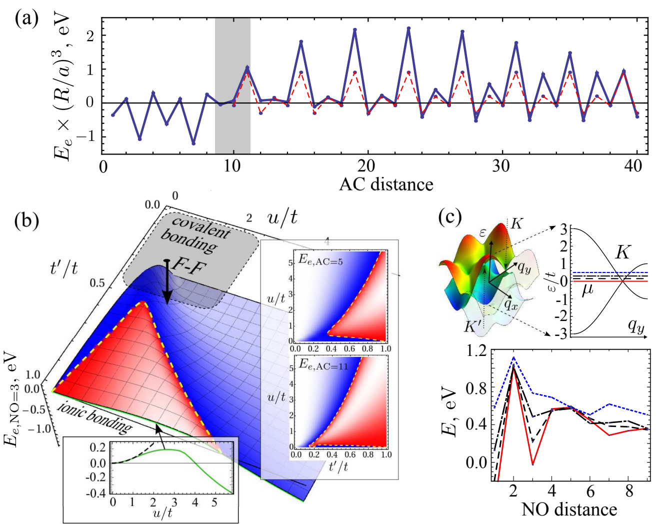

Figure 2: Adsorbate-adsorbate interaction energy for different scattering strengths and distances. (a) Crossover from strong to weak coupling limits with distance: at short distances the minima occur when adsorbates are on different sub-latices [odd sites along AC, in Fig. 1(d)]; at R_C of about AC=10 (shaded area) the phase abruptly changes, and the minima occur when adsorbates are at the same sub-lattice sites (even site along AC). The dashed line is the weak coupling limit. (b) The A-A interaction as a function of t' and u at NO=3 distance between the adsorbates. The parameters for two F adsorbates are indicated by an arrow and "F-F". The bottom sub-panel shows $t' = t$ dependence (solid curve), which start quadratically in u (dashed curve). The right sub-panel shows interaction energy for AC=5 and AC=11. (c) The A-A interaction energy as a function of distance for different chemical potentials $\mu/t = 0, 0.15, 0.3, 0.5$: solid (red), dashed, dash-doted, and doted (blue) lines respectively. The top sub-panel shows the values of μ relative to graphene's spectrum.

Coulomb interaction can be well approximated [35] by $E_C(\mathbf{R}) = e^2Z^2/4\pi\varepsilon_0 r$, where Z is the effective charge drawn to the adsorbate complex obtained from DFT calculations ($Z \approx -0.39$ for F). As we will see shortly, the screening due to the fourth and the fifth terms (1) do not alter the $1/R$ dependence in $E_C(\mathbf{R})$ and can be ignored. As an example, we consider the system of two F adsorbates. To examine $E_C(\mathbf{R})$ we performed a DFT calculation [30] in which C atoms were restricted to their original (clean, flat graphene) positions, while the positions of the F atoms were allowed to relax [see "DFT, flat" curve in Fig. 1(c)]. Each F attracts negative charge. The restriction (to flat graphene) enforces sp^2 hybridization for the C atom under each F atom making the C-F bond mostly ionic. It also eliminates possible elastic deformation of graphene sheet around both F atoms, as well as electron scattering due to the second and the third terms in (1). The C pz orbitals under F's remains part of the graphene's π-system, i.e., $t'_{n,0} = t$ and $u_{n,0} \to 0$. The electron exchange that can originate from the fifth term of (1) is still present in this configuration. However, by comparing $E_C(\mathbf{R})$ and "DFT, flat" results in Fig. 1(c) we conclude that it does not contribute substantially to the A-A interaction, even for the high values of Z in this example.

We now investigate the role of the u and t' terms in $E_e(\mathbf{R})$. We compute the interaction energy $E(\mathbf{R})$ between to F's with fully relaxed DFT [30], in which we allow deformation of graphene ["DFT" curve in Fig. 1(c)]. We also evaluate the TB [34] interaction energy $E_e(\mathbf{R})$ based on the first three terms of (1). The TB $E(\mathbf{R})$ is denoted as "TB with Coulomb" in Fig. 1(c). The values of u and t' found earlier for a single F were used. The DFT and TB curves show remarkable agreement at distances starting from the third nearest neigbour order, NO=3, [see Fig. 1(d)]. Larger deviations at NO=1 and NO=2 distances can be attributed to a combination of local deformation in graphene-adsorbate system and to direct overlap of fluorine electron orbitals not accounted for by Hamiltonian (1). To understand the physics of $E_e(\mathbf{R})$ we will examine an analytical solution for this system in two limiting cases.

The interaction energy $E_e(\mathbf{R})$ can be obtained by summing all $\mathbf{R}$-dependent diagrams for the electron free energy using linked cluster expansion [36]. The expression for $E_e(\mathbf{R})$ can be rearranged to

$$E_e(\mathbf{R}) = 2\int d\mathbf{r}d\mathbf{r}'V_1(\mathbf{r})V_2(\mathbf{r}')J(\mathbf{R}+\mathbf{r}-\mathbf{r}'), \quad (2)$$

$$J(\mathbf{r}_{ij}) \equiv J_{ij}(\mathbf{r}_{ij}) = \int \frac{d\omega}{2\pi} G^{(0)}_{ij}(i\omega,\mathbf{r}_{ij})G_{ji}(i\omega,\mathbf{r}_j\mathbf{r}_i). \quad (3)$$

Here $V_{1(2)}$ is the scattering potential due to the second and third terms of Hamiltonian (1), $\mathbf{r}_{ij} = \mathbf{r}_i - \mathbf{r}_j$ is the distance between two lattice sites, one at sub-lattice i and the other at j. The indexes i, j take the value of A and B when $\mathbf{r}_i$ is on two different sub-lattices of graphene [1, 37]. The function $G^{(0)}_{ij}(i\omega,\mathbf{r})$ is the bare equilibrium Green's function [37] and $G_{ij}(i\omega,\mathbf{r}_i\mathbf{r}_j)$ is the dressed equilibrium Green's function which contains multiple scattering events [36]. The limits $u = 0$, $t' \to 0$ and $t' = t$, $u \to \infty$ are equivalent and represent a strong scattering system: in both cases an electron cannot enter the adsorbate site(s). A weak scattering limit can be illustrated by the system with $u \ll t$, $t' = t$. We will focus on the $t' = t$ case and set $V_n(\mathbf{r}) = uV_C\delta(\mathbf{r} - \mathbf{R}_n)$, where V_C is the volume of graphene's primitive cell. We are interested only in $G(i\omega, \mathbf{R}_1\mathbf{R}_2)$, which can be found exactly

$$G(i\omega,\mathbf{R}_1\mathbf{R}_2) = \mathfrak{N}(i\omega,\mathfrak{F}(i\omega,\mathbf{R}))G^0(i\omega,\mathbf{R})\mathfrak{N}(i\omega,0), \quad (4)$$

where $\mathfrak{N}(i\omega, X) = [1 - uV_CG^0(i\omega,0)/\sqrt{2} - X]^{-1}$ and $\mathfrak{F}(i\omega,\mathbf{R}) = (uV_C)^2G^0(i\omega,\mathbf{R})\mathfrak{N}(i\omega,0)G^0(i\omega,-\mathbf{R})/2$. Matrix products are implied where ij-indexes are dropped.

When the scattering is small, $u \to 0$, $G \to G^{(0)}$ and we obtain $E_e(\mathbf{R}) = 2u^2V_C^2J^{\mathrm{RKKY}}_{ij}(\mathbf{R})$, recovering the standard RKKY range function for graphene [37]

$$J_{ij}^{\mathrm{RKKY}}(\mathbf{R})=\frac{(-1)^{i-j+1}\sqrt{3}}{3^{i-j}2^{6}\pi t a^{4}}\frac{1+\cos[\mathbf{R}(\mathbf{K}-\mathbf{K}')+(2\theta+\pi)\delta_{i\neq j}]}{(R/a)^{3}}. \tag{5}$$

where we use $A-A=0$ and $A-B=1$ for i,j indexes.

Unlike magnetic scattering in RKKY, which is weak in most cases, scattering of electrons on adsorbates can be strong. In the limit $u\to\infty$, the frequency integral in Eq. (3) is given predominantly by $\omega\sim v/R$. As a result, at large (but finite) distances we can use $\mathfrak{N}(i\omega,\mathfrak{F}(i\omega,\mathbf{R}))\mathfrak{N}(i\omega,0)\sim -1/\mathfrak{F}(i\omega,\mathbf{R})$ and obtain

$$J_{ij}(\mathbf{R})\approx\frac{(-3)^{i-j}\pi\sqrt{3}t}{2^{6}(R/a)}\frac{1+\cos\mathbf{R}(\mathbf{K}-\mathbf{K}')}{1+\cos[\mathbf{R}(\mathbf{K}-\mathbf{K}')+(2\theta+\pi)\delta_{ij}]}. \tag{6}$$

In some cases $\mathfrak{F}\sim 1+\cos[\mathbf{R}(\mathbf{K}-\mathbf{K}')+2\theta+\pi]\to 0$ and the frequency integration is determined by the renormalization factor $\mathfrak{N}(i\omega,0)^{2}$. In this case $J_{AA}(\mathbf{R})\approx -\sqrt{3}ta[1+\cos\mathbf{R}(\mathbf{K}-\mathbf{K}')]/4R$. The interaction energy given by (6) and (2) is shown in the inset of Fig. 1c along with with the numerical TB result for two F's. Deviations of the analytical result at short distances are due to approximate integration and the use of linear dispersion in the analytical estimates.

The interplay between the two distinct regimes, (i) weak coupling from Eq. (5), and (ii) strong coupling from Eq. (6), can be used to modify the adsorbate-adsorbate interaction. Note that the A-A interaction in these limits have opposite phases, c.f. prefactors $(-1)^{i-j+1}$ and $(-3)^{i-j}$. At finite scattering strength and $\mathbf{R}\to\infty$ the the range function J in Eq. (3) approaches the weak coupling limit. This can be most easily seen in the TB calculations for two F adsorbates placed at AC sites [see Fig. 2(a)]. The crossover between the two limiting regimes takes place gradually over a substantial distance. However, the phase associated with sub-lattice oscillations noted above changes abruptly at some R_C [see the shaded region in Fig. 2(a)]. The value of R_C can be estimated from the denominator of $\mathfrak{N}(i\omega,\mathfrak{F}(i\omega,\mathbf{R}))$. We obtain $R_C/a\sim u/t$.

To investigate the interplay of weak and strong coupling we perform TB calculations [34] for different values of t' and u. We use the sign of the A-A interaction at a specific distance R, e.g. NO=3, as an indication of the interaction regime [see Fig. 2(b)]. The weak interaction regime is observed at small-to-intermediate u and for a range of t' values (depending on $\mathbf{R}$). At large values of u, for $t'\to t$, and finite distances the interaction converges to the strong coupling limit [see Eq. 6] as expected. The region with t' and u, which is typical of covalently bound adsorbates [indicated (approximately) by a shaded box in Fig. 2(b)], is near the transition boundary. As a result, small changes in the bonding characteristics, e.g., due to changes in internal structure of an adsorbed molecule, can potentially lead to dramatic modification of the A-A interaction at different distances. This effect, combined with the recently proposed directed motion of the adsorbates [15] can provide control of interest in a variety of applications, such as chemical sensing and patterning. Ionically bound adsorbates are expected to leave the carbon π-conjugated network intact as $t'\to t$, interacting predominantly in the weak coupling regime. The change of sign between the strong and week coupling regime will also take place for multivalent adsorbates, e.g., oxygen [15]. In that case the oscillatory behavior of the A-A interaction in the weak coupling limit will be similar to that for magnetic RKKY interaction when spin impurities reside in between the nodes of the lattice [37]. In the strong scattering limit the renormalization factors $\mathfrak{N}$ will change the range function as it happened in the example of the monovalent adsorbates above. As a result, the interplay between strong and weak coupling limits can be utilized to control the A-A interaction in a similar fashion.

Finally, we investigate the role of the chemical potential, μ. Changes due non-zero μ in $G^{(0)}G^{(0)}$ are not significant up to very high chemical potentials where the scattering processes are no longer confined to well-defined Dirac cones [see the top sub-panel in Fig. 2(c)]. The renormalization factors in (4), however, are more sensitive. As a result, chemical potential can be used to alter the A-A interaction in the strong coupling regime. As an example, we consider the system of two F adsorbates as before. In Fig. 2(c) we plot $E(\mathbf{R})$ for several values of μ from 0 to $0.5t$ that can be achieved by back-gating or chemical doping. Substantial changes in the A-A interaction can be seen even for relatively small values of μ: e.g., in the example in Fig. 2(c) the minimum of the interaction energy shifts from NO=3 to NO=6 as μ increases.

We have demonstrated that the dominant contribution to the A-A interaction is due to scattering of π-electrons on the distortions cased by the adsorbates. The proposed tight-binding model gives excellent agreement with the DFT calculations. Mechanisms to control the A-A interaction at different distances has been proposed.

This work was supported in part by the ONR and by DOE at LANL under Contract No. DE-AC52-06NA25396. Computer resources were provided by the DoD HPCMP.

---

[*] Electronic address: d.solenov@gmail.com

[†] Electronic address: kirill@lanl.gov

[1] A. K. Geim and K. S. Novoselov, Nature Mat. 6, 183 (2007).

[2] S. Das Sarma, S. Adam, E. H. Hwang, and E. Rossi, Rev. Mod. Phys. 83, 407 (2011).

[3] T. O. Wehling, K. S. Novoselov, S. V. Morozov, E. E. Vdovin, M. I. Katsnelson, A. K. Geim, and A. I. Licht-

enstein, Nano Lett. 8, 173 (2008).

[4] J. M. Englert, C. Dotzer, G. Yang, M. Schmid, C. Papp, J. M. Gottfried, H.-P. Steinruck, E. Spiecker, F. Hauke, and A. Hirsch, Nature Chem. 3, 279 (2011).

[5] D. W. Boukhvalov and M. I. Katsnelson, J. Phys.: Condens. Matter 21, 344205 (2009).

[6] S. M. Kozlov, F. Vines, and A. Gorling, Adv. Mat. 23, 2638 (2011).

[7] E. Rotenberg, The Electronic Properties of Adsorbates on Graphene (Springer-Verlag Berlin Heidelberg, 2012), pp. 93134.

[8] T. O. Wehling, M. I. Katsnelson, and A. I. Lichtenstein, Phys. Rev. B 80, 085428 (2009).

[9] T. O. Wehling, S. Yuan, A. I. Lichtenstein, A. K. Geim, and M. I. Katsnelson, Phys. Rev. Lett. 105, 056802 (2010).

[10] X. Liu, C. Z. Wang, M. Hupalo, W.-C. Lu, P. A. Thiel, K. M. Ho, and M. C. Tringides, Phys. Rev. B 84, 235446 (2011).

[11] A. V. Krasheninnikov and R. M. Nieminen, Theor. Chem. Acc. 129, 625 (2011).

[12] P. Lambin, H. Amara, F. Ducastelle, and L. Henrard, Phys. Rev. B 86, 045448 (2012).

[13] T. O. Wehling, M. I. Katsnelson, and A. I. Lichtenstein, Chem. Phys. Lett. 476, 125 (2009).

[14] A. M. Suarez, L. R. Radovic, E. Bar-Ziv, and J. O. Sofo, Phys. Rev. Lett. 106, 146802 (2011).

[15] D. Solenov and K. A. Velizhanin, Phys. Rev. Lett. 109, 095504 (2012).

[16] C.-J. Shih, G. L. C. Paulus, Q. H. Wang, Z. Jin, D. Blankschtein, and M. S. Strano, Langmuir 28, 8579 (2012).

[17] A. V. Shytov, D. A. Abanin, and L. S. Levitov, Phys. Rev. Lett. 103, 016806 (2009).

[18] V. V. Cheianov, O. Syljuasen, B. L. Altshuler, and V. Falko, Phys. Rev. B 80, 233409 (2009).

[19] V. V. Cheianov, V. I. Falko, O. Syljuasen, and B. L. Altshuler, Solid State Comm. 149, 1499 (2009).

[20] S. Kopylov, V. Cheianov, B. L. Altshuler, and V. I. Falko, Phys. Rev. B 83, 201401(R) (2011).

[21] L. F. Huang, T. F. Cao, P. L. Gong, Z. Zeng, and C. Zhang, Phys. Rev. B 86, 125433 (2012).

[22] P. Giannozzi and S. Baroni and N. Bonini and M. Calandra and R. Car and C. Cavazzoni and D. Ceresoli and G. L. Chiarotti and M. Cococcioni and I. Dabo and A. Dal Corso and S. Fabris and G. Fratesi and S. de Gironcoli and R. Gebauer and U. Gerstmann and C. Gougoussis and A. Kokalj and M. Lazzeri and L. Martin- Samos and N. Marzari and F. Mauri and R. Mazzarello and S. Paolini and A. Pasquarello and L. Paulatto and C. Sbraccia and S. Scandolo and G. Sclauzero and A. P. Seitsonen and A. Smogunov and P. Umari and R. M. Wentzcovitch, J.Phys.: Condens. Matter **21**, 395502 (2009).

[23] M.-T. Nguyen, R. Erni, D. Passerone, Phys. Rev. B 86, 115406 (2012)

[24] K.H. Lau, Solid State Comm. 28, 757 (1978).

[25] P. Peyla and C. Misbah, Eur. Phys. J. B 33, 233 (2003).

[26] The next nearest-neighbor hopping [1, 27] does not change the A-A interaction substantially and we will ignore it.

[27] V. M. Pereira, F. Guinea, J. M. B. Lopes dos Santos, N. M. R. Peres, and A. H. Castro Neto, PRL 96, 036801 (2006).

[28] Different parametrizations of TB are in principle possible [8], however the chosen parametrization is best suited for our purpose.

[29] Electron spin does not have any substantial effect on the adsorbate-adsorbate interaction between non-magnetic adsorbates. It will add a factor of 2 in all integrals over the electron's momentum.

[30] DFT calculations: Quantum Espresso [22]; Perdew-Burke-Ernzerhof (PBE) exchange-correlation; Generalized gradient approximation (GGA); Vanderbilt ultrasoft psuedopotentials; Semi-empirical dispersion terms (DFT-D) [31–33]; Rectangular 12-by-12 graphene supercells; Inter-layer spacing of 15 Å.

[31] S. Grimme, Journal of Computational Chemistry **27**, 1787 (2006).

[32] V. Barone, M. Casarin, D. Forrer, M. Pavone, M. Sambi, A. Vittadini, Journal of Computational Chemistry **30**, 934 (2009).

[33] S. Grimme, Wiley Interdisciplinary Reviews: Computational Molecular Science **1**-2, 211 (2011)

[34] TB calculations: a number of different sizes of the supercell were investigated: 20x20, 50x50, 70x70 primitive cells of graphene; 57x57 momentum points were used.

[35] In the case of a more complex adsorbates the charge distribution in the molecule [the last term of Eq. (1)] has to be taken into account at shorter distances, which will alter the $1/R$ dependence.

[36] G. D. Mahan, Many-Particle Physics (Kluwer Academic, New York, 2000).

[37] M. Sherafati and S. Satpathy, Phys. Rev. B 83, 165425 (2011).